APPLICATION OF TRANSPORT TECHNIQUES TO THE ANALYSIS OF NERVA SHADOW SHIELDS

M. A. Capo and S. L. Anderson

Westinghouse Electric Corporation

Astronuclear Laboratory

A radiation shield internal to the NERVA* nuclear rocket reactor is required to limit the neutron and photon radiation levels at critical components located external to the reactor. These radiation levels are unusually severe since the reactor is designed to operate at a power level of 1511 thermal megawatts for a total time of 10 hours. The internal shield is currently being designed to meet radiation criteria developed by Aerojet Nuclear Systems Company for minimum shield weight missions. The criteria are specified in terms of the required radiation levels at a plane tangent to the dome of the nuclear subsystem and at several critical locations in the engine.

To design a minimum weight shield internal to the NERVA Nuclear Subsystem, the capabilities and limitations of the analytical techniques must be clearly understood. To further this understanding, an in-depth study was performed in which both one and two dimensional discrete ordinate techniques were applied to the analysis of several shadow shield experiments. These experiments were performed at the Westinghouse Astronuclear Experimental Facility on the PAX reactor which was modified to simulate the R-1 reactor, an upgraded version of the NRX nuclear rocket technology series of reactors tested at Nevada during the past six years.

Two significantly different shield mockups were analyzed. In one experiment, the internal shield material called BATH (a composite mixture of boron carbide, aluminum and titanium hydride) was mocked up by alternating thin sheets of titanium, Boral, aluminum and polyethylene. In another experiment a borated steel-liquid hydrogen shield was mocked up by alternating layers of borated steel and polyethylene.

The two-dimensional discrete ordinates code, DOT-IIW, was employed to calculate 16 group (11 fast and 5 thermal) neutron fluxes internal to the shield mockups. These fluxes were processed by the NAGS code to obtain photon sources throughout the assembly. Photon flux distributions were obtained by employing these sources in fixed source, thirteen group, DOT calculations. An S_8 angular quadrature was employed. Approximately 8000 mesh cells were utilized to describe the two-dimensional geometry.

One-dimensional analysis was accomplished by means of the ANISN code. Briefly, this technique employed 29 (16 neutron and 13 photon) energy groups simultaneously in one problem with the photon source generation process treated as a downscattering interaction from one of the neutron groups to one of the photon groups. Two approximations to account for transverse leakage were investigated: 1) the addition of a DB^2 correction to the energy-dependent absorption cross section, and, 2) a "void" streaming correction for geometrical regions containing no material.

Based on the comparisons between the experimental and calculated neutron and photon radiation levels, the following conclusions were noted:

1) the ability of the two-dimensional discrete ordinates code, DOT-IIW to predict the radiation levels internal to and at the surface of the shield mockups was clearly demonstrated,
2) internal to the BATH shield mockups, the one-dimensional technique predicted the axial variation of neutron fluxes and photon dose rates; however, the magnitude of the neutron fluxes was about a factor of 1.8 lower than the two-dimensional analysis and the photon dose rate was a factor of 1.3 lower,

---

* NOTE: The Nuclear Engine for Rocket Vehicle Application Program (NERVA) is administered by the Space Nuclear Systems Office, a joint office of the U. S. Atomic Energy Commission and the National Aeronautics and Space Administration. Aerojet Nuclear Systems Company, as prime contractor for the engine system, and Westinghouse Electric Corporation as subcontractor for the nuclear subsystem, are developing a nuclear propulsion system for space applications.

3) internal to the borated steel-liquid hydrogen shield mockup, the application of the DB^2 correction significantly over estimated the attenuation of the shield by as much as a factor of 30.

INTRODUCTION

A radiation shield internal to the NERVA nuclear rocket reactor is required to limit the neutron and photon radiation levels at critical components located external to the reactor. These radiation levels are unusually severe since the reactor is designed to operate at a power level of 1511 thermal megawatts for a total time of 10 hours.

The internal shield is currently being designed to meet radiation criteria developed by Aerojet Nuclear Systems Company[1] for minimum shield weight missions. The criteria are specified in terms of the required radiation levels at a plane tangent to the dome of the nuclear subsystem and at several critical locations in the engine.

To design a minimum weight shield internal to the NERVA Nuclear Subsystem, the capabilities and limitations of the analytical techniques must be clearly understood. To further this understanding, an in-depth study was performed in which both one and two dimensional discrete ordinate techniques were applied to the analysis of several shadow shield experiments.

Both one and two dimensional analysis techniques were investigated since economics and schedular considerations can necessitate the employment of the less accurate one-dimensional approach. For example, in the design of a minimum weight shield system, the need for extensive parametric studies is obvious. Yet, to perform analyses of this type with the two-dimensional discrete ordinates technique is often not feasible. In addition, situations do occur in which the employment of the two-dimensional approach is not necessary and the one-dimensional technique will suffice. Thus, it is imperative, from a practical standpoint, that the shield analyst be well aware of the capability of the one-dimensional approach for analyzing complex shield configurations. Without this knowledge, the analyst can neither apply the technique to applicable situations with any degree of confidence; nor, when forced to employ the approach, realize the possible margin of error in the analytical results.

The experiments were performed on the PAX[2] reactor which has been modified to simulate the R-1 reactor, which is the upgraded flight version (increased operating lifetime, power level, and thrust) of the previous NRX nuclear rocket technology series of reactors, tested at Nevada during the past six years.

Figure 1 is a photograph of the PAX reactor in the test cell with a mockup nozzle in place. To accomplish the experiments described in this paper, the mockup nozzle was removed from the reactor, and slab mockups of the shields were placed at the aft end of the core along with appropriate support structure.

Two different types of shield mockups were employed in the experiments. In one experiment, the NERVA internal shield material called BATH (a composite mixture of boron carbide, aluminum and titanium hydride) was mocked up by alternating thin sheets of titanium, Boral, aluminum and polyethylene. (The BATH material was chosen for use in the NERVA reactor due to its efficiency as a combination neutron-photon shield material.) The second type of shield mockup consisted of alternating layers of borated steel and polyethylene foam to simulate a borated steel-liquid hydrogen internal shield.

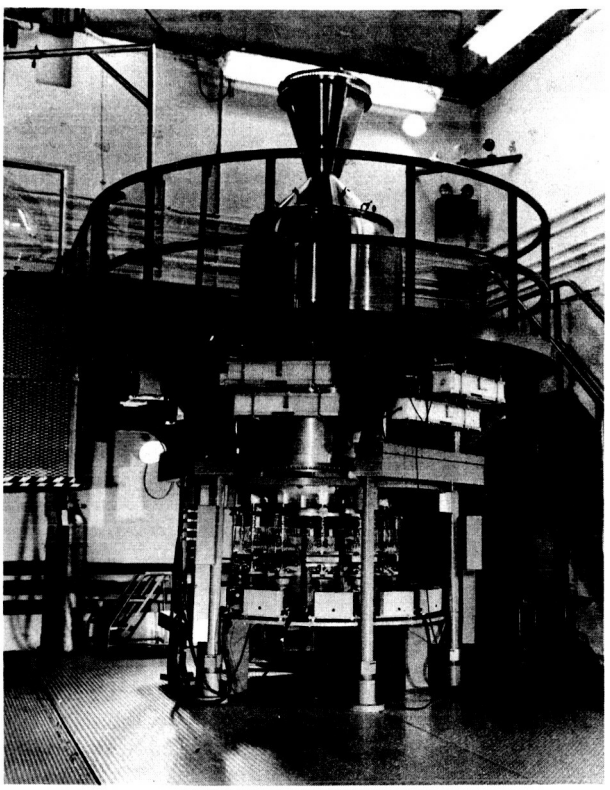

FIGURE 1
THE PAX REACTOR WITH MOCKUP NOZZLE IN PLACE

EXPERIMENTAL DETAILS

A schematic diagram of the PAX-G0C reactor assembly is shown in Figures 2 and 3. Figure 2 shows a sectional view through the reactor axis, whereas Figure 3 depicts a top view of the system. Figure 2 essentially displays a cross sectional view of the major reactor regions as mocked up in the R,Z discrete ordinate transport code analysis. Major regions are indicated by title in the figure, i.e., the reactor core, reflector, and other hardware. From Figure 3, it is observed that the shield materials were actually in the form of square slabs extending beyond the reactor radius which is illustrated by the dotted circle.

Experimental data were obtained both internal to and external to the BATH shield mockup and the borated steel-liquid hydrogen shield mockup located at the aft end of the core as shown in Figure 2. This paper discusses only the internal environment data. Additional detailed analysis is provided in Reference 2.

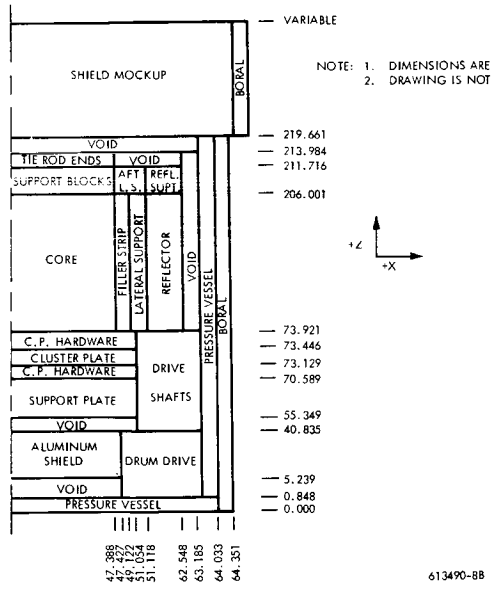

PAX-G0C REACTOR MOCKUP FOR SHIELD EXPERIMENTS
(SECTIONAL VIEW THROUGH THE REACTOR AXIS)

FIGURE 2

FIGURE 3

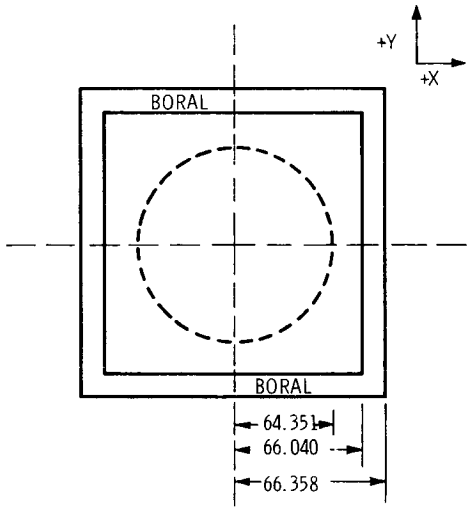

NOTE: 1 DIMENSIONS ARE IN CM.
2 DRAWING IS NOT TO SCALE.

613490-7B

PAX-G0C REACTOR MOCKUP FOR SHIELD EXPERIMENTS (TOP VIEW)

A schematic drawing of a BATH shield mockup is shown in Figure 4. The axial thickness of this mockup is about 19.5" and the mass thickness is 109 gm/cm^2. Experimental data were obtained in the ten dosimeter slots shown in Figure 4. Each dosimeter slot was $\sim$ 0.95 cm in thickness. Also shown in Figure 4 is a typical BATH module which consists of slabs of titanium, aluminum, boral and polyethylene in the proper proportions to simulate the actual BATH material composition ($\sim$ 70% aluminum, 24% titanium hydride, and 6% boron carbide by volume.)

Figure 5 illustrates the borated steel-liquid hydrogen steel mockup shield assembly consisting of alternating layers of steel and polyethylene (to simulate the liquid hydrogen). The axial thickness of this mockup is about 35 inches, but the mass thickness is only about 117 gm/cm^2. Slots were cut in the polyethylene slabs for the purpose of placing dosimeters internal to the mockups at the locations indicated.

The experimental data taken internal to the mockups was obtained in the form of radial distributions of equivalent neutron flux and photon dose rate at various axial locations within the mockup. These axial locations are defined by the dosimeter slots illustrated in Figures 4 and 5. The radiation levels internal to the mockups were obtained using passive dosimetry techniques. The neutron flux was measured by means of sulfur pellets (E>2.9 MeV), cadmium covered U-238 foils (E>1.5 MeV), and by dysprosium difference techniques (E<0.4 eV). The photon dose rate was measured with CaF_2 thermoluminescent detectors (TLD).

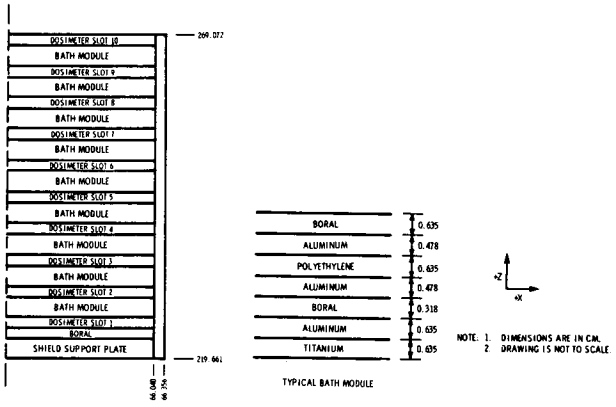

BATH SHIELD MOCKUPS USED FOR PAX-GOC EXPERIMENTS

FIGURE 4

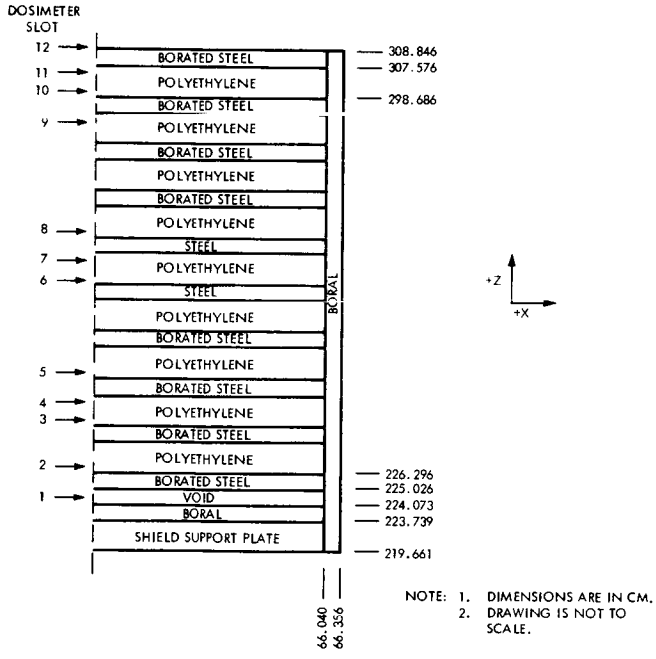

BORATED STEEL-LIQUID HYDROGEN SHIELD MOCKUP USED FOR PAX-GOC EXPERIMENTS

FIGURE 5

METHOD OF ANALYSIS

Two-Dimensional Discrete Ordinate Technique

The two-dimensional discrete ordinate analytical procedure employed to calculate the neutron and photon radiation levels internal to both shield mockups is shown schematically in Figure 6. In addition to depicting the flow of information throughout the calculation, Figure 6 illustrates the type of information derived from each computation as well as the sequence of calculations.

Basically, the neutron transport analysis was carried out in two parts utilizing the DOT-IIW S_n transport code.[3] The first part of the procedure was an eigenvalue calculation on the basic reactor assembly. The basic reactor is defined in this study as that portion of the assembly which extends from the pressure vessel dome (Z=0.00) to an axial plane located a short distance into the shield mockup (Z dependent on the shield mockup being analyzed). From the eigenvalue problem, the neutron flux distributions throughout the basic reactor assembly were obtained, as well as an angular and energy dependent boundary source, based on the angular flux distributions at the midplane of the shield support plate (Z=221.536). Using this boundary source as a coupling mechanism, a second DOT-IIW problem was employed to obtain flux distributions throughout the shield geometry. By performing the analysis in two parts, a rather large computer cost savings was realized. The eigenvalue calculations on the basic reactor required multiple (typically 5-10) outer iterations due to the criteria for source convergence. However, since the analysis of the shield geometry employed a fixed boundary source, only a single outer iteration was needed. Had the shield configurations been analyzed along with the basic reactor in a single problem, the multiple outer iterations necessary for eigenvalue convergence would, of course, have encompassed a much larger number of spatial mesh points; and the running time would have been increased accordingly. (In addition, since two BATH shield mockups were analyzed which were merely different thicknesses of the same material, it was possible to employ one boundary source for both shield geometries; and, by eliminating one reactor calculation, to effect a further cost savings. This analysis is presented in Reference 2.)

From Figure 6, it can be observed that the starting point (calculational sequence 1) is the generation of neutron cross sections. To accomplish this, the appropriate atom densities and other required data are input to the GAMB1T[4] code. GAMB1T calculates the 16 group (11 fast, five thermal), region dependent, macroscopic, P_0 transport corrected neutron cross sections for use in the discrete ordinate codes. These cross sections were weighted over region dependent 155 fine group spectra which had been generated for use in prior PAX-G0 analysis. Since the magnetic tape containing these spectra is not generally available, it would be necessary for an analyst attempting to reproduce this study to employ the GAMB1T-ANISN[5]-ANISIG[6] linkage, described in Reference 7, in his cross section generation procedure.

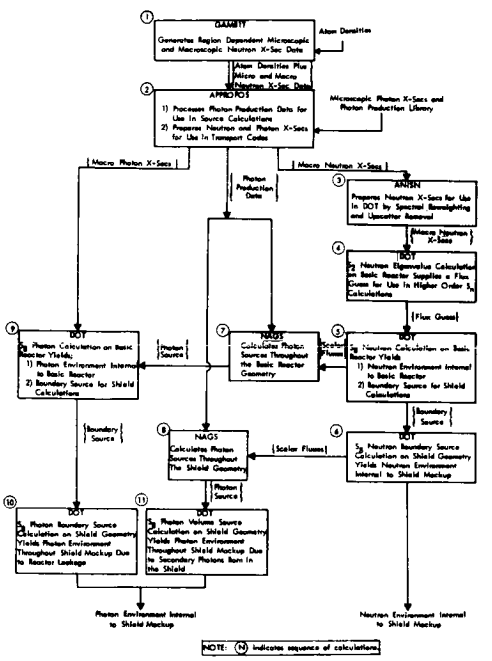

FIGURE 6

FLOW CHART FOLLOWED TO CALCULATE NEUTRON AND PHOTON ENVIRONMENT INTERNAL TO THE PAX-G0C SHIELD MOCKUPS

Although Figure 6 indicates (calculational sequence 2) that the macroscopic neutron cross sections flow through the APPROPOS[8] code, this step was unnecessary for the two-dimensional analysis. Macroscopic neutron cross sections are indeed required as input to the APPROPOS code. However, these cross sections are only used to generate data for use in simultaneous neutron-photon calculations. Analyses of this type will be discussed later in connection with the one-dimensional analysis of the PAX-G0C shield experiments. Thus, in the case of the two-dimensional analysis, the macroscopic neutron cross section output from APPROPOS was identical to the input.

Prior to application in the two-dimensional S_n analysis, the macroscopic neutron cross section output from APPROPOS[8] is input to two ANISN one-dimensional S_n transport problems - one radial and one axial problem (calculational sequence 3). First, by running a radial calculation characteristic of the reactor regions centered about the core midplane and an axial calculation including all regions located on the reactor axis, an initial flux guess for use in the two-dimensional S_n calculations was obtained. Second, the ANISN problems were employed to effect upscatter removal from the neutron cross sections By removing upscatter from the cross sections, a large cost savings is realized in the subsequent two-dimensional DOT-IIW problems. Furthermore, since the upscatter removed cross sections were weighted over the region dependent flux calculated by ANISN, it is believed that no significant loss of accuracy was incurred by employing the upscatter removed cross sections in the DOT-IIW calculations.

As was stated earlier, the neutron transport analysis employed P_0 transport corrected cross sections in a 16 energy group problem. The final eigenvalue calculation on the basic reactor configuration was preceded by a calculation which employed S_2 angular quadrature. It has been recommended[3] that a computer cost savings is achieved by running a low order quadrature DOT-IIW problem to obtain a good flux guess for the calculation employing the higher order quadrature. Using the S_2 flux guess in the S_8 problem allows eigenvalue and pointwise flux convergence in a minimum of computer time.

The boundary source to be used as input to the S_n calculations on the shield geometry was obtained from the basic reactor problem by saving, on magnetic tape, the angular flux for each of the three axial mesh intervals describing the shield support plate. The angular flux obtained in the central axial interval was then input from tape to the appropriate shield problem. In order to obtain a valid boundary source for input to subsequent calculations, it is imperative for the angular flux at the boundary source location to accurately reflect the presence of the particular shield configuration under consideration. For this reason, the basic reactor geometry was extended beyond the axial plane at which the boundary source was obtained.

The reader will recall from Figure 4 that each BATH module was constructed by laminating a series of titanium, aluminum, polyethylene, and boral plates. This configuration could not be represented as a heterogeneous shield because the mesh sizing requirements (see Reference 3) coupled with the large number of physical regions resulted in a problem whose size is beyond the capabilities of the CDC6600 computer system with 128K storage (91,000 data locations available after DOT-IIW program is loaded). Thus, it was necessary either to relax the mesh sizing requirements or to homogenize the individual BATH modules. Of these two alternatives, the latter was chosen for the analysis reported herein. In the case of the laminated borated steel-polyethylene configuration shown in Figure 5, however, each lamination was included explicitly in the shield geometry problem.

Both the experimental and analytical results internal to the various shield mockups are presented in this paper in terms of an "equivalent neutron flux" based on the response of the following detectors; sulfur pellets ($E>2.9$ MeV), cadmium covered U-238 foils ($E>1.5$ MeV), and bare minus cadmium covered dysprosium foils ($E<0.4$ eV). Briefly, the experimentally determined equivalent neutron flux is obtained by dividing the measured saturated activity of the given detector by a constant, C, based on an average cross section for the neutron interaction being considered. The analytical equivalent neutron flux is obtained by calculating the saturated activity and then dividing by the same constant, C, in the DOT-IIW problems. Thus, the comparisons presented in this paper are essentially based on measured and calculated activities and, for relative comparison purposes, the effective neutron interaction cross section used to determine the constant, C, is rather immaterial. (A detailed discussion of the generation and use of activation cross sections for analysis of this type is given in Reference 9).

The analysis of the photon environment internal to the various shield mockups followed a procedure which was similar and, through the source terms, intimately related to the internal neutron environmental analysis. As in the case of neutrons, the overall problem was divided into two parts; a basic reactor calculation and a shield calculation (calculation sequences 9 and 10). However, unlike the neutron analysis, a single boundary source calculation on the shield geometry was not sufficient. In addition to the boundary source calculation of leakage through the shield mockup, it was necessary to perform a fixed volume source calculation in order to account for secondary photons produced via neutron interactions in the shield itself (calculational sequence 11).

The region dependent photon cross sections employed in the internal analysis were generated by the APPROPOS code using microscopic cross section data from the GAMLEG[8] code as input. As can be seen from Figure 6, fixed volume distributed source terms for use in the analysis of the basic reactor as well as the shield mockups were calculated via the NAGS[10] data processing code. Briefly, the NAGS code combines neutron scalar flux distributions obtained from a prior neutron analysis of the geometry of interest with neutron interaction cross sections from GAMBIT and a photon production library from APPROPOS to produce a spatial and energy dependent photon source throughout the problem geometry.

All of the photon transport problems to determine the photon environment internal to the basic reactor as well as the various shield mockups employed a P_1 scattering cross section approximation with 13 energy groups and S_8 angular quadrature.

The experimentally determined photon dose rates internal to the shield mockups were reported as Mrad(C)/hr-watt. The data were obtained by calibrating the response of a CaF_2 thermoluminescent detector (TLD) with a known source of Co-60 radiation. The analytical response was obtained by converting the calculated energy flux distributions to dose rate by means of standard energy-dependent flux-to-dose conversion factors.

There are several distinct differences between the neutron and photon internal analysis which may be summarized as follows. There were, of course, basic differences in cross sections in the analysis. The neutron analysis employed P_0 transport corrected cross sections, whereas, a full P_1 cross section set was incorporated into the photon analysis. The neutron analysis of the basic reactor was an eigenvalue problem, while the photon calculation utilized a fixed distributed source based on converged neutron fluxes from the eigenvalue case. Finally, although a single boundary source computation was sufficient to obtain neutron flux distributions throughout the shield mockups, for photons it was necessary to employ, in addition to the boundary source calculation, a fixed distributed source problem to account for secondary photons born in the shield regions. Only by summing the results of the boundary source problem and the fixed source problem was it possible to obtain the total photon radiation levels internal to the shield mockups.

In the BATH shield analysis described above, 3550 mesh cells (in a 50 radial by 71 axial array) were employed in the reactor geometry, and 5350 (in a 50 radial by 107 axial array) were employed in the shield geometry, for a total of 8400 mesh cells. In the borated steel-liquid hydrogen shield analysis, 3850 mesh cells (in a 50 radial by 77 axial array) were employed in the reactor geometry, and 4200 (in a 50 radial by 84 axial array) were employed in the shield geometry, for a total of 8050 mesh cells.

One-Dimensional Discrete Ordinate Technique

Both the BATH shield and the borated steel-liquid hydrogen shield mockups were analyzed using the ANISN one-dimensional discrete ordinate transport code. The axial mesh allocation employed in the ANISN problems was identical to that employed in the pertinent DOT-IIW problem.

The analysis of the shield mockups was carried out via the simultaneous neutron-photon calculational technique incorporated into the APPROPOS - ANISN system, schematically shown in Figure 7.

As can be seen from Figure 7 the neutron cross sections employed in the analysis were obtained from the GAMBIT code, while the photon cross section data were generated by the GAMLEG code. With the exception of the reactor core, there is a one-to-one correspondence between the axial region atom densities used in the one and two dimensional codes. Cross sections for the core region were obtained by volume averaging those in the 15 radial core zones shown employed in the two-dimensional code.

As shown in Figure 7, the respective neutron and photon basic cross sections from GAMBIT and GAMLEG were input to the APPROPOS code, wherein, they were combined with photon production data to yield a single transfer matrix for use in the simultaneous neutron-photon analysis. Briefly, this technique employed 29 energy groups (16 neutron groups and 13 photon groups) with the photon source generation process treated as a downscattering interaction from one of the neutron groups to one of the photon groups. For example, if, in the calculation, a hypothetical particle scatters from energy group 16 to energy group 24, the physical analog would be the capture of a group 16 neutron with the corresponding generation of a photon with energy characteristic of group 24.

It should be noted that the cross sections utilized in the one-dimensional discrete ordinate analysis included a P_1 expansion in the scattering matrix. However, the values of the P_1 component existed for only groups 17 through 29. For the neutron groups (1 through 16), the P_1 component was input as zero. Thus, in effect, the neutron analysis employed P_0 transport corrected cross sections, whereas, the photon calculations employed P_1 cross sections. Thus, from a cross section standpoint, the one-dimensional analyses were entirely compatible with the two-dimensional calculations.

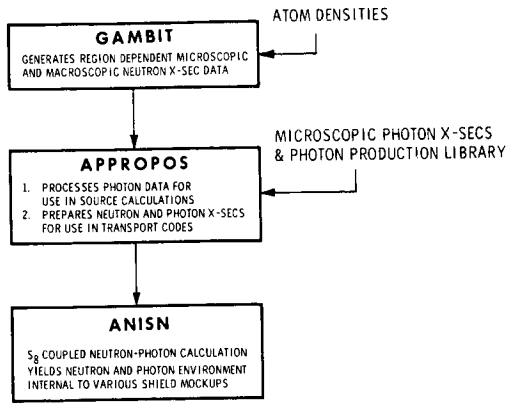

FLOW CHART FOR ONE-DIMENSIONAL ANALYSIS OF PAX-GO SHIELD MOCKUPS 613490-11B

FIGURE 7

As in the case of the two-dimensional analysis, the ANISN calculations employed S_8 angular quadrature and solutions were based on both eigenvalue and point-wise flux convergence. Likewise, both neutron and photon response functions utilized for the experimental comparisons were identical to those employed in the two-dimensional analysis.

When applying the ANISN code to perform radiation transport analysis, it is customary to include a DB^2 correction to the absorption cross sections in order to estimate the effect of transverse leakage from the slab system on the overall attenuation properties of the medium in question. In addition to this transverse leakage correction, the WANL version of the ANISN[5] code includes an option whereby a void streaming correction may be employed to account for transverse leakage in regions which contain no material.

In this study, both the DB^2 correction and the void streaming correction were employed in the analysis of the BATH shield mockup. The lateral dimensions of the slabs of material which comprised the shield mockup was utilized in the generation of these transverse leakage terms. In the analysis of the borated steel-liquid hydrogen mockup, the employment of a void streaming correction was not necessary. However, the DB^2 correction was, at first, applied. Unfortunately, when the DB^2 correction was employed, the analytical results were obviously in error. Thus, the calculation was repeated with the DB^2 correction removed. The results of this second analysis were more reasonable, but still not satisfactory. The comparison of the calculations with and without the transverse leakage correction (to be presented in the next section) point out a rather serious problem area which must be taken into account when applying the one-dimensional discrete ordinate technique to the R-1 type reactor, particularly in the areas of hydrogen plena.

RESULTS OF ANALYSIS

Before discussing comparisons in detail, it is of interest to review some data which demonstrates that, in the area of overlap, the eigenvalue calculation on the basic reactor geometry and the boundary source calculation on the shield geometry yield equivalent results. The reader will recall that the model of the basic reactor employed in the analysis extended to the midplane of the second BATH module. Thus, both the reactor calculation and the shield calculation encompassed, in part, an area which included a portion of the shield support plate, a 1/8 inch boral plate and dosimeter slots 1 and 2 as well as the aforementioned amount of the BATH mockup.

A comparison of analytical results from the basic reactor calculation with those from the BATH shield coupled calculation is presented in Figure 8. The choice of dosimeter slot 1 as the point of comparison was based solely on convenience. The ratios presented are typical of those observed from the boundary source location up to some distance into the first BATH module. As one might expect, the presence of subsequent BATH modules in the coupled calculation was reflected in the results obtained in dosimeter slot 2 and beyond. Thus, comparisons of the type presented tend to diverge in the vicinity of the second shield module.

In general, the comparisons presented in Figure 8 are quite favorable for both neutrons and photons and, thus, lend credence to the coupled calculation as a technique for analyzing complex shield systems.

FIGURE 8

COMPARISON OF RESULTS OF SINGLE CALCULATION WITH RESULTS OF COUPLED CALCULATION IN DOSIMETER SLOT 1 IN THE BATH SHIELD MOCKUP

	SINGLE CALCULATION	COUPLED CALCULATION	RATIO: COUPLED/SINGLE
SULFUR RESPONSE			
R = 0 cm	3.324(4)	3.397(4)	1.022
R = 30 cm	2.551(4)	2.606(4)	1.022
R = 60 cm	5.764(3)	5.899(3)	1.023
U-238 RESPONSE			
R = 0 cm	1.306(5)	1.345(5)	1.030
R = 30 cm	1.007(5)	1.035(5)	1.028
R = 60 cm	2.344(4)	2.416(4)	1.031
Dy RESPONSE			
R = 0 cm	2.191(2)	2.313(2)	1.056
R = 30 cm	1.846(2)	1.933(2)	1.047
R = 60 cm	1.090(2)	1.091(2)	1.001
CaF_2 RESPONSE			
R = 0 cm	1.018(0)	9.928(-1)	0.9752
R = 30 cm	7.679(-1)	7.475(-1)	0.9734
R = 60 cm	2.542(-1)	2.495(-1)	0.9815

NOTE: Numbers in parentheses refer to powers of ten.

It should be pointed out that, since these data are intended solely as a comparison of the two linked calculations, the CaF_2 response does not include the effects of secondary photons born in the shield materials. Rather, only those photons which are born within the basic reactor geometry and subsequently leak through the boundary source plane are included.

Comparisons of calculated and measured response of sulfur pellets are presented in Figures 9 and 10 as a function of axial position internal to the BATH and BSS-LH_2 shield mockups, respectively. In these and subsequent figures, the reference "0" position is located at the top of the reactor assembly as shown in Figure 2. The experimental data as well as the DOT-IIW calculated results illustrated in Figures 9 and 10 are characteristic of a traverse taken along the centerline of the two shield mockups. The analytical results obtained with the ANISN code, being one-dimensional in nature, are not representative of a unique radial position within the shield mockup.

From Figure 9, it is seen that internal to the BATH shield mockup the agreement between the measurements and the DOT-IIW calculation is excellent. No significant differences between the analytical and experimental results are observed. In addition, the results of the one-dimensional analysis indicate that, qualitatively speaking, the ANISN code predicts the falloff of the sulfur threshold flux through the BATH mockup quite well. The magnitude of the one-dimensional results are, however, lower than the two-dimensional analytical data by a factor which ranges from 1.8 in dosimeter slot 1 to 1.6 in dosimeter slot 10. These ratios are typical of the centerline to average ratios observed in the two-dimensional analysis. Hence, for this geometric situation, the one-dimensional analysis is essentially in good agreement with the two-dimensional analysis.

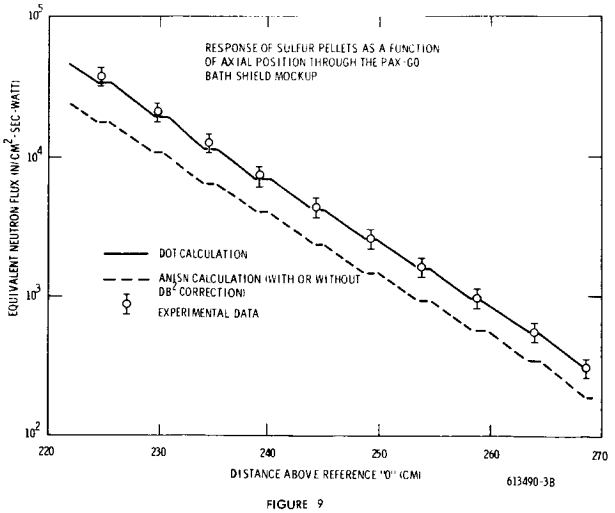

FIGURE 9

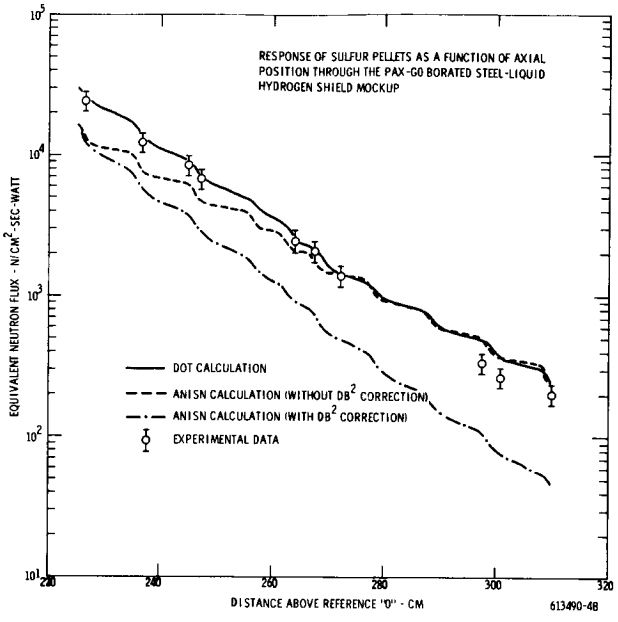

FIGURE 10

From Figure 10, it is noted that internal to the BSS-LH_2 shield mockup the agreement between the measured and DOT-IIW calculated sulfur response is, in general, quite good. However, for axial location beyond Z=280 cm a disagreement which progressively worsens with penetration distance is evident. This disagreement is apparently due to a change in the slope of the calculated attenuation curve for Z>280 cm. A slope change of this nature is not explainable on a physical basis, but may be explained in terms of a calculational deficiency.

A close examination of the calculations performed on the BSS-LH_2 mockup showed that the above mentioned anomaly was observed only for the highest neutron energy group in the calculation. It was further observed that the radius over which the anomaly occurred was governed only by the first tier of polar angles in the S_8 quadrature. Thus, the calculation near the top of the mockup and near the centerline involved an essentially uncollided transport of the forward directed flux from the boundary source plane to the top of the shield. Due to the large physical size of the mockup in question, a calculation of this type represents a severe test of the analytical approach. It is possible that, in the area of the calculational anomaly, the angular flux solutions became oscillatory in nature and the negative flux fix-up routine incorporated into the DOT-IIW code resulted in the observed slope change and the corresponding overpredictions.

Returning to Figure 10, it is noted that the one-dimensional analytical results are presented for calculations both with and without the DB^2 adjustment to the cross sections. It may be noted that when the DB^2 correction is employed the slope through the shield mockup is too steep (ANISN results underpredict measurements by a factor of 1.7 at dosimeter location 1, but by a factor of 4.0 at location 12). Conversely, the slope of the attenuation curve resulting from calculations in which the DB^2 adjustment was not employed is clearly too shallow. Thus, it is evident that the form of the transverse leakage approximation presently incorporated into the ANISN code may, in some circumstances lead to erroneous results. These erroneous results are, of course, indicative of the presence of low density regions (polyethylene) in the shield mockup. In the higher density regions (steel plates) adverse affects of the DB^2 adjustment are not observed.

It is further apparent from Figure 10 that there should be some form of transverse leakage approximation that will result in the proper slope through the mockup. The proper transverse leakage approximation might be arrived at either by making an adjustment to the transverse dimension that is used to calculate the leakage terms or by employing some form of region as well as energy dependent buckling correction. However, both of these improvements might prove to be impractical. In order to apply either an adjustment to the transverse dimension or a region dependent buckling, it is necessary to know a priori the leakage characteristics of the given system. Information of this type may be obtained only from a detailed two-dimensional analysis of the system in question.

Comparisons of the measured and one and two-dimensional calculated cadmium covered U-238 response data (E>1.5 MeV data) presented in Reference 2 displayed characteristics similar to the sulfur data described above.

Comparisons of measured and calculated response of bare minus cadmium covered dysprosium foils are presented as a function of axial location within the BATH and BSS-LH_2 mockups in Figures 11 and 12, respectively. As in the case of the sulfur data, the DOT-IIW analytical results and the measurements were obtained at the centerline of the shield system.

From Figure 11, it is of interest to note that, although the qualitative behavior of the one and two-dimensional analytical results internal to the BATH mockup are quite similar, the two-dimensional approach tends to overpredict the measurements while the results of the one-dimensional analyses agree fairly well with the experimental data. This apparent anomaly in the analytical results may be due to two competing processes which, in the one-dimensional analyses, negated one another, thus, producing the favorable results.

From the schematic diagram of the BATH shield mockup shown in Figure 4, it is clear that once the radiation leaking from the basic reactor penetrates a short distance into the shield, incident thermal neutrons have been attenuated to the point of insignificance; and the thermalization of fast and intermediate energy neutrons has become the dominant mechanism of thermal flux production. Furthermore, it may be noted that most of the thermalization in the BATH mockup is due to the presence of polyethylene. Now, it will be recalled that in the analysis of the BATH mockup, the individual BATH modules were treated as homogeneous regions. Thus, the principle thermalizing media (polyethylene) was dispersed throughout the module. Recall that in the actual experimental configuration the polyethylene was separated from the dosimeter slots and sandwiched between

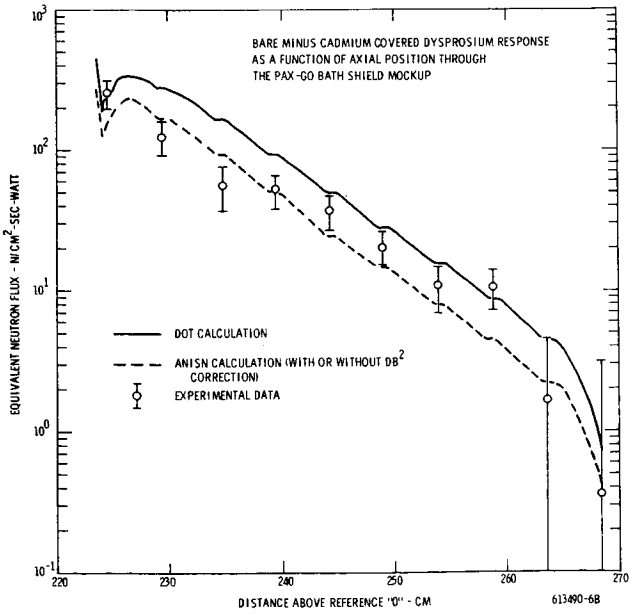

FIGURE 11

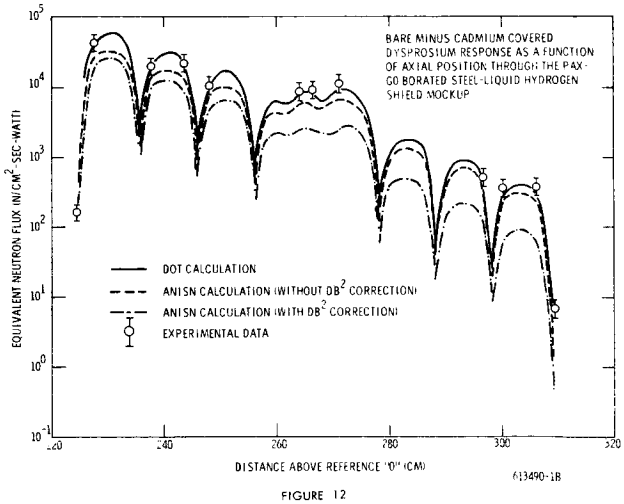

FIGURE 12

boral plates. Thus, from a calculational standpoint, the homogenization process, which not only moves thermalizing material close to the detector location but also disperses the boron poison, tends to produce an overprediction of the thermal flux within the dosimeter slots. Coupled with this overestimate of thermal flux induced by the homogenization process is the fact that the one-dimensional approach, in the slab configuration, inherently underpredicts the centerline value. It is evident, therefore that this inherent underprediction acted in conjunction with the overestimation induced by the homogenization process to produce the results shown in Figure 11. Despite this error in thermal flux calculations caused by homogenizing the BATH modules, it is evident from the qualitative behavior of the analytical results depicted in Figure 11, that the DB^2 adjustment did not have any adverse effect on the thermal flux calculations internal to the BATH mockup.

From Figure 12, on the other hand, it is apparent that, while the two-dimensional results agree quite favorably with the measurements, the one-dimensional calculations do not. The ANISN calculation which employs the DB^2 adjustment clearly underpredicts the measurement to a larger degree than does the calculation which did not include the DB^2 correction. It should be noted that the thermalization process is intimately related to the fast flux distributions within the mockup. As a result of this dependence, the transverse leakage effects observed in Figure 12 reflect changes noted in the fast flux distributions (See Figure 10) which were induced by the DB^2 adjustment.

Comparisons of calculated and measured response of CaF_2 thermoluminescent dosimeters are presented in Figures 13 and 14 as a function of axial position internal to the BATH and BSS-LH_2 shield mockups, respectively. Again, the two-dimensional analytical results as well as the experimental data are representative of a centerline traverse.

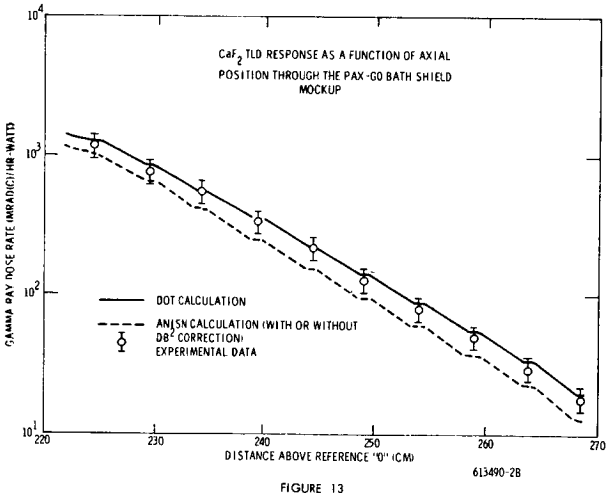

FIGURE 13

Figure 13 illustrates a comparison similar to that shown in Figure 9 in connection with the sulfur pellet data. The agreement between the two-dimensional analytical results and the measurements is excellent. The one-dimensional calculated data employing the transverse leakage adjustment reproduces the experimental gradient through the mockup with a good deal of accuracy. The analytical results are, however, low by a factor of about 1.3 throughout the mockup. As in the case of fast neutrons, the factor of 1.3 is typical of the centerline to average ratios observed in the two-dimensional analysis of the BATH shield.

From Figure 14, it is seen that the agreement between the DOT-IIW calculations and the measurements is somewhat less than desirable. At present, these differences are not completely understood. However, it is believed that the two-dimensional calculation accurately predicts the gradient of the photon dose rate across the mockup. It is further evident, from Figure 14, that although the data obtained from the ANISN calculation without the transverse leakage adjustment indicate an erroneous gradient, the overall results are not too unreasonable. On the other hand, the results obtained from the calculations in which the DB^2 correction was employed are very poor. It is interesting to note that the DB^2 correction in the polyethylene regions reduces the direct radiation component to such an extent that the secondary photons in the steel plates effect a significant increase in the photon dose rate in and around these plates. Clearly, the DB^2 correction used in ANISN cannot be employed to accurately predict the photon transport in low density media.

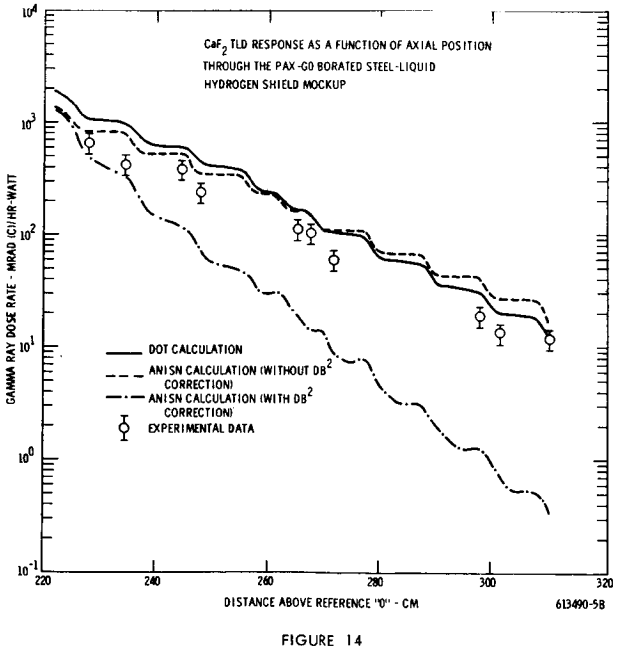

FIGURE 14

CONCLUSIONS

Based on the foregoing comparisons between the measured and calculated neutron and photon radiation levels internal to the BATH and the BSS-LH_2 shield mockups, the following conclusions were noted:

1) The ability of the two-dimensional discrete ordinates code, DOT-IIW to predict the radiation levels internal to the shield mockups was clearly demonstrated.

2) The capability and feasibility of coupling two-successive transport problems at an arbitrary "boundary source" plane was demonstrated. This boundary source feature is extremely important in that a judiciously chosen boundary source may, for a given reactor, be applied to parametric shield studies in such a way that the analysis is facilitated and the overall cost greatly reduced.

3) The one-dimensional calculation inherently underpredicted centerline radiation levels internal to the slab shields. Thus, caution should be exercised when estimating maximum or "peak" radiation levels from the results of a one-dimensional analysis. As an example of this tendency toward underprediction, recall that internal to the BATH shield mockup the ANISN analytical results were consistently lower than either the DOT-IIW calculated or experimentally measured centerline values. For fast neutrons, ANISN results were low by a factor of about 1.8 and, for photons by a factor of 1.3.

4) Problem areas attributable to the use of a transverse leakage approximation were identified in the one-dimensional analytical results. The error induced by employing the transverse leakage approximation is largest for regions in which the actual leakage is relatively large, i.e., low density regions; and, as might be expected, in regions with either large transverse dimensions or high density material these effects are somewhat mollified. Because of this transverse leakage problem, the photon attenuation of the BSS-LH_2 shield mockup was overestimated by a factor of 30.

5) The two-dimensional discrete ordinates approach has been shown to accurately predict radiation levels internal to slab mockups of shadow shields; while, at the same time, serious problem areas associated with the application of the one-dimensional S_n method to the analysis of these slab configurations have been identified. Nevertheless, for many applications the employment of the one-dimensional approach is economically attractive. Thus, further studies aimed at a better understanding of the effects of employing a transverse leakage approximation are certainly warranted.

REFERENCES

1. RN-S-0557, "Radiation Exposure Limitations for Shielded NERVA Engine Components," Aerojet Nuclear Systems Company, April, 1970.
2. WANL-TME-1912, "Nuclear Subsystem Shielding Provision Study Experiments," August, 1970.
3. WANL-TME-1982, "User's Manual for the DOT-IIW Discrete Ordinates Transport Computer Code," R. G. Soltesz, and R. K. Disney, December, 1969.
4. WANL-TME-1969, "Second Version of the GAMBIT Code," G. Collier, G. Gibson, L. L. Moran, R. K. Disney, and R. S. Kaiser, November, 1969.
5. WANL-TMI-1967, "Revised WANL ANISN Program User's Manual," R. G. Soltesz, April, 1969.
6. ANISIG User's Manual (To be Published).
7. WANL-TME-2689, "The Evaluation of the WANL Integrated Nuclear, Radiation and Shielding Standard Design Method (WISDM)," to be published.
8. WANL-PR(LL)-034, "Nuclear Rocket Shielding Methods, Modification, Updating, and Input Data Preparation," Volume 3, "Cross Section Generation and Data Processing Techniques," R. G. Soltesz, et al, August, 1970.
9. American Nuclear Society Paper Presented at the 1969 Winter Meeting, "Neutron Flux Spectra Measurements with Energy Dependent Activation Foils and Comparison with Multigroup Reaction Rate Calculations." S. Salah, W. D. Rankin, and V. S. Oblock.
10. WANL-PR(LL)-010, "Synthesis of Calculational Methods for the Design and Analysis of Radiation Shields for Nuclear Rocket Systems," Volume 7, R. K. Disney, R. G. Soltesz, and S. L. Zeigler, June, 1967.